EXTRACTION OF SIGNALS IN THE PRESENCE OF STRONG NOISE: CONCEPTS AND EXAMPLES

RALPH v. BALTZ
Institut für Theorie der Kondensierten Materie
Universität Karlsruhe, D–76128 Karlsruhe, Germany *

1. Introduction

In experimental physics, communication electronics and other technical disciplines one is often faced with the challenge of detecting weak signals $s(t)$ which are buried under noise $n(t)$. Assuming a linear superposition, the total signal is

$$f(t) = s(t) + n(t), \quad \text{S/N} = 10\log(\frac{P_s}{P_n}) \text{ dB}. \tag{1}$$

S/N denotes the signal to noise ratio and P_s, P_n, respectively, are the power of the signal and noise in the bandwidth of the detector. Here, noise is short for all types of broadband disturbances masking the information which is contained in $s(t)$.

Depending on the character of the signal the human ear is capable to extract signals which are 6dB under the noise level. Good quality broadcast requires at least S/N= +20dB whereas experiments often struggle with S/N= −40dB or less.

In this article, signals are always understood as (multicomponent) functions of time. Signal processing with respect to spatial variables is the field of *image–processing* and *pattern–recognition.*

The plan of this contribution is twofold. In chapters 2-4, general concepts of signal processing and statistical properties of noise are reviewed, whereas chapt. 5 gives a selection of examples with sketchy solutions. Chapter 6 contains some closing remarks on Quantum Noise. For general references see Refs.[1](a-c). The only book which – to my knowledge – conforms with the title of this report is an old book by Wainstein and Zubakov[2] with emphasis on radar signals.
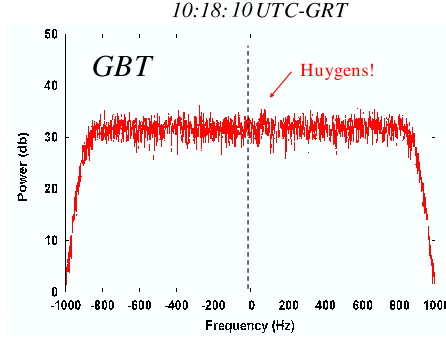
---

* http://www.tkm.uni-karlsruhe.de/personal/baltz/

Figure 1.   Huygens signal received at the Green Bank Telescope (GBT), USA[4](c).

2. Signals

A recent spectacular example of weak signal detection is the direct reception of the Huygens signal by some very large radio telescopes[3](a,b). Due to an error in the configuration of the receiver on the Cassini relay the complete data of the Huygens Doppler wind–experiment during descend on Saturn's moon Titan would otherwise be lost[4](a,b). (For some technical details see the JPL–report[5] and appendix A). Refs.[6](a,b) provide two additional examples of weak–signal–detection with amateur equipment:
– radio communication via reflections from the moon (power < 1kW),
– detection of a Mars orbiter relay on 437MHz (1W, isotropic radiation).
     The natural mathematical basis for the representation and processing of signals is the complex *Fourier–transformation* (FT)[7](a),[1]

$$\text{FT:} \quad \boxed{f(t) = \int_{-\infty}^{\infty} F(\omega)\, e^{-\mathrm{i}\omega t}\, \frac{d\omega}{2\pi}, \quad F(\omega) = \int_{-\infty}^{\infty} f(t)\, e^{\mathrm{i}\omega t}\, dt.} \tag{2}$$

In practice, FT is always performed over finite time– and frequency–intervals. To remove artefacts from the ends of the time–integration interval a window–function $w(t)$ is used which smoothly tends to zero near the endpoints. A convenient window–function is the *Hamming–window*[7](b)

$$w_H(t) = \frac{1}{2} \left(1 + \cos\frac{\pi t}{T}\right) \theta(T^2 - t^2).$$

Moreover, a time and frequency dependent *windowed-FT* can be defined from which – remarkably – the complete signal $f(t)$ can be reconstructed

$$F(\omega, \tau) \;=\; \int_{-\infty}^{\infty} f(t')\, w(t' - \tau)\, e^{\mathrm{i}\omega t'}\, dt', \tag{3}$$

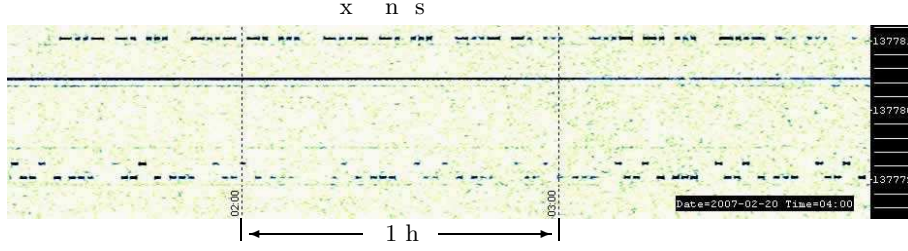[1] Fourier–transformed functions are denoted by capitals, if suitable.

Figure 2. Screen shot of slow speed telegraphy signals (60s per dot) on 137 kHz received in north Germany by sliding FT. Upper trace: station WD2XNS (east coast USA, radiated power ≈ 1 W) sending Morse–Code "xns". Horizontal axis: time, vertical axis: frequency (total span ≈ 2 Hz). From Ref.[8](a).
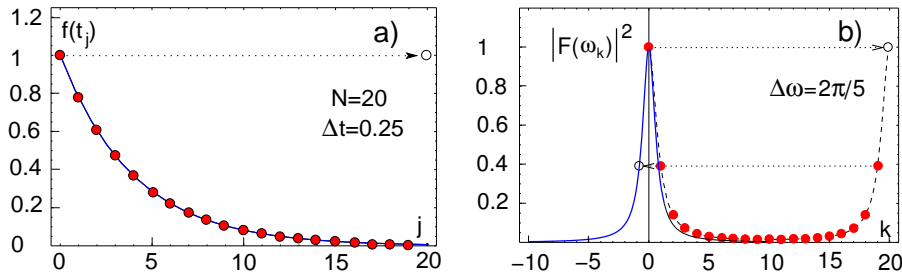

Figure 3. Discrete Fourier–Transformation.

$$f(t) = \frac{1}{w(0)} \int_{-\infty}^{\infty} F(\omega, t)\, e^{-i\omega t}\, \frac{d\omega}{2\pi}, \qquad (4)$$

$$F(\omega) = \frac{1}{W} \int_{-\infty}^{\infty} F(\omega, \tau)\, d\tau\,, \quad W = \int_{-\infty}^{\infty} w(\tau) d\tau. \qquad (5)$$

Fig. 2 diplays an example of a time dependent FT which is used in amateur radio to detect very weak signals transmitted on 137 kHz across the Atlantic[8](a-c).

Today, signal processing is mainly numerically done, first by
– *Analogue–Digital Conversion* (ADC): $f(t) \rightarrow f_j = f(t_j), \quad t_j = j\Delta t$, where Δt is the *sampling–time* and $j = 0, 1, \ldots, (N-1)$.
– Then, FT is performed in discretized form (DFT) for both $f(t)$ and $F(\omega)$,

$$\text{DFT:} \quad \boxed{f_j = \sum_{k=0}^{N-1} F_k\, e^{-i\frac{2\pi}{N}jk}, \quad F_k = \frac{1}{N} \sum_{j=0}^{N-1} f_j\, e^{i\frac{2\pi}{N}jk}.} \qquad (6)$$

Time span: $T = N\Delta t$. Frequency resolution: $\Delta\omega = 2\pi/T$, $\omega_k = k\Delta\omega$.
– Technically, FT is performed using standard *Fast–Fourier* routines[9].
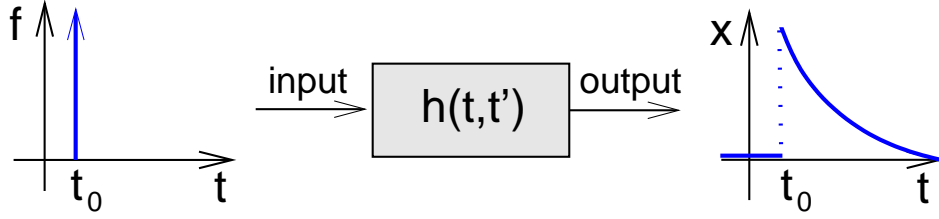
Figure 4. Block diagram of a linear system transforming $f(t)$ into $x(t)$.

f_j as well as F_k are periodic functions of j and k (mod N) which may cause "aliasing problems", see Fig. 3. Very often, a *symmetric form* of the k–periodicity interval with respect to $k = 0$ is used (as in solid state theory): $|\omega| < \Omega = \pi/\Delta t$ (Nyquist–rate).

Remarkably, the analogue signal $f(t)$ can be perfectly reconstructed from the discretized signal f_j provided $f(t)$ is *band–limited*[10].

Bernstein–Theorem:

if:
$$f_j = f(j\Delta t), \ j = 0, 1, \ldots N - 1, \text{ and}$$

$$F(\omega) \equiv 0 \text{ for } |\omega| > \Omega, \ \Omega = \pi/\Delta t,$$

then:
$$f(t) = \sum_{j=0}^{N-1} f_j \mathrm{sinc}(\Omega t - j\pi), \quad \mathrm{sinc}(x) = \frac{\sin(x)}{x}. \ (*)$$

Support of $f(t)$: extends from $-\infty$ to ∞,

derivatives: exist to all orders.

In principle, the Bernstein–result (*) could be used for *Digital–Analogue–Conversion* (DAC). In practice, however, DAC is performed holding $f(t) = f_j$ =const in the time–interval $t_j \leq t < t_{j+1}$ ("histogram") with subsequent smoothening by an analogue low pass filter (RC–circuit).

3. Linear Systems

A *linear System* (LS) – as sketched in Fig. 3 – is a device which linearly transforms an input signal $f(t)$ into an output $x(t)$,

$$\text{Linear System:} \quad \boxed{x(t) = \int_{-\infty}^{\infty} h(t, t') \, f(t') \, dt'.} \tag{7}$$

$h(t, t')$ is called the (impulse) *Response Function*, system–function or just "filter". [2]

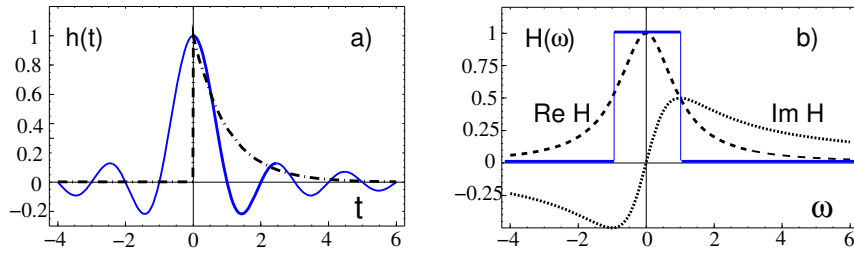[2] $f(t)$, $x(t)$, $h(t, t')$ may have several components or may be fields.

Figure 5.   Ideal low–pass filter (full lines) and relaxator (dashed/dotted lines).

Basic properties are[1]:

– time–invariance: $h(t, t') = h(t - t')$,

– TI+causality: $h(t - t') \equiv 0, \quad t' > t$,

– in ω–space: $X(\omega) = H(\omega)\, F(\omega)$,

– analyticity: $H(\omega)$ analytic function of complex ω for $\mathrm{Im}\,\omega > 0$
                (time–invariant causal systems).

Examples:

a) unit–system: $h(t) = \delta(t)$, $H(\omega) = 1$,

b) delay–line: $h(t) = \delta(t - T)$, $H(\omega) = e^{\mathrm{i}\omega \mathrm{T}}$,

c) relaxator: $h(t) = e^{-\gamma t}\, \Theta(t)$, $H(\omega) = \dfrac{1}{\gamma - \mathrm{i}\omega}$,

d) ideal low–pass: $h(t) = \dfrac{\Omega}{\pi}\, \mathrm{sinc}(\Omega t)$, $H(\omega) = \Theta(\Omega^2 - \omega^2)$,
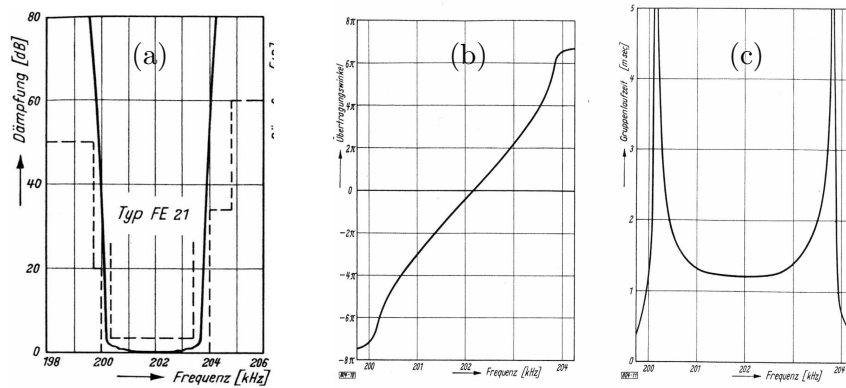

Figure 6.   Mechanical filter Telefunken FE 21 [14 coupled, torsional steel resonators; conversion of the electric signal into mechanical vibrations and back to an electrical signal]. (a) $H(\omega)$, (b) phase $\Phi(\omega)$ of $H(\omega)$, (c) pulse delay time $\tau = \frac{\partial \Phi}{\partial \omega}$. From Ref[11].
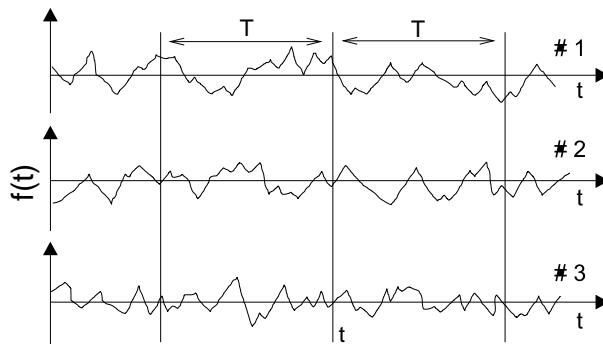
Figure 7. Three members of a statistical ensemble of a random signal.

Fig. 5 displays the system functions for c) and d). A relaxator acts as a *Low–Pass–Filter* (LPF) which can be realized as a RC–circuit ("integrator"). Example (d) refers to an *ideal LPF*. As $h(t) \neq 0$ for $t < 0$, such a filter is acausal and can be only realized as a digital filter. Fig. 6 shows the characteristics of a *mechanical filter* which was used in high–end commercial and military short–wave reveivers.

Clearly, extraction of weak, but spectrally narrow signals, can be successfully done by reducing the bandwidth of the receiver ("filtering"), see Figs. 1,2.

Today, signal processing is mainly numerically performed by first digitizing the signal by an ADC, FT, filtering, inverse FT, and DAC to back to the time–domain. Apparently, digital filters may (mathematically) violate causality.[3] Nevertheless, digital filters can be much more powerful than analogue filters.

4. Noise

4.1. STOCHASTIC DESCRIPTION

There are signals which are so irregular ("erratic") that only a probabilistic description is possible. But noise is not always a hindrance of signal detection, in some cases, the noise itself is the signal, e.g., in the *Hanbury–Brown & Twiss effect*[12] or studies on electron kinetics[13].

Basic rules are[14]:

– time average:
$$\overline{x(t)} = \lim_{T \to \infty} \frac{1}{2T} \int_{-T}^{T} x(t + t') \, dt',$$

---

[3] Digitizing the analogue signal during time T, data–storage, FT, etc. needs a finite time so that the analogue output can never appear before the input signal ended.
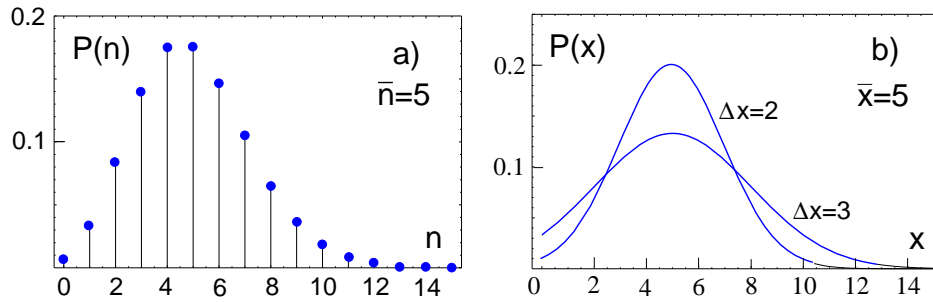
Figure 8. a) Poissonian and b) Gaussian–distributions[14](a,b).

– ensemble average: $\quad \langle x(t)\rangle = \lim\limits_{N\to\infty} \dfrac{1}{N} \sum\limits_{k=1}^{N} x_k(t),$

– ergodicity (+stat.): $\quad \langle x(t)\rangle = \overline{x(t)} \ (=0),$

– probability dist.: $\quad P(x,t) > 0, \quad \int P(x,t)\,dx = 1,$

$$\langle x^k(t)\rangle = \int P(x,t)\,x^k\,dx, \quad k = 0,1,2,\dots$$

– deterministic signal: $\quad P(x,t) = \delta(x - \xi(t)),\ \xi(t)$ prescribed function.

A complete description of a random process $x(t)$ requires the knowledge of the probability of the whole process, i.e. $P[x(t)]$. This is equivalent to the knowledge of $P(x;t)$, joint probability $P(x_1, x_2; t_1, t_2)$, etc.

Central limit theorem:
If x is the sum of many independent, random variables then $P(x)$ becomes a *Gaussian* (irrespective of the statistics of the individual variables)

$$P_{\mathrm{G}}(x) = \frac{1}{\sqrt{2\pi\sigma}}\, e^{-\frac{(x-\bar{x})^2}{2\sigma}}, \quad \sigma = (\Delta x)^2.$$

Poissonian distribution:
The *Poissonian* $P_{\mathrm{P}}(n)$ is the limiting case $(p \ll 1, n \ll N)$ of a *Binomial distribution*. The probability that an event characterized by probability p occurs n times in N trials reads

$$P_{\mathrm{B}}(n) = \binom{N}{n} p^n (1-p)^{N-n} \to P_{\mathrm{P}}(n) = e^{-\bar{n}}\frac{\bar{n}^n}{n!}, \quad \bar{n} = pN.$$

4.2. CORRELATION FUNCTIONS

In addition to the probability distribution functions a second set, named *correlation functions* will be useful[14](a,b)

$$C_{\mathrm{ff}}(t_1, t_2) \;=\; \overline{f(t+t_1)\, f(t+t_2)} = \iint P(f_1, f_2; t_1, t_2)\, f_1\, f_2\, df_1\, df_2. \quad (8)$$

Basic properties are[14]:

– steady state: $\quad C_{\mathrm{ff}}(t_1, t_2) = C_{\mathrm{ff}}(|t_1 - t_2|) = \int C_{\mathrm{ff}}(\omega)\, e^{-\mathrm{i}\omega(t_1 - t_2)}\, \dfrac{d\omega}{2\pi},$

– inequality: $\quad |C_{\mathrm{ff}}(t)| < C_{\mathrm{ff}}(t=0), \quad t = t_1 - t_2,$

– quadratic average: $\quad \langle [f(t)]^2 \rangle = \int C_{\mathrm{ff}}(\omega)\, \frac{d\omega}{2\pi},$

– power spectrum: $\quad C_{\mathrm{ff}}(\omega) = \frac{1}{2T} |F(\omega)|^2 > 0,$

– white noise: $\quad C_{\mathrm{ff}}(\omega) = \text{const}, \quad C_{\mathrm{ff}}(t) \propto \delta(t).$

$$\text{Wiener–Khinchine–Th:} \quad \boxed{\; C_{\mathrm{ff}}(\omega) = \frac{1}{2T} |F(\omega)|^2 > 0. \;} \qquad (9)$$

$F(\omega)$ of a stationary, random process $f(t)$ may not exist. This is circumvented by using a time cut–off, i.e. setting $f(t) \equiv 0$ for $|t| > T$ and performing the limit $T \to \infty$ at the end.[4]

Filtering of a random signal:

Filtering $f(t)$ with correlation function $C_{\mathrm{ff}}(\omega)$ leads to an output signal with changed correlations

$$\text{Filtered Noise:} \quad \boxed{\; C_{\mathrm{xx}}(\omega) = |H(\omega)|^2\, C_{\mathrm{ff}}(\omega). \;} \qquad (10)$$

In particular, filtering of white noise creates correlations of finite duration. Numerous examples of student experiments on noise and correlation can be found in the American Journal of Physics, e.g. Refs.[15](a-c).

An example of an apparatus to measure correlations of the electromagnetic field in the optical region is the *Michelson interferometer*, see Fig. 9. For a box–shaped intensity profile of total width $\Delta\omega$ centered at $\omega_0 > 0$, the complex optical coherence function becomes

$$G(t_2 - t_1) = \langle \mathcal{E}^{(-)}(t_2)\mathcal{E}^{(+)}(t_1) \rangle = I_0\, \frac{\Delta\omega}{2}\, e^{-\mathrm{i}\omega_0(t_2 - t_1)}\, \mathrm{sinc}\left(\frac{\Delta\omega(t_2 - t_1)}{2} \right).$$

---

[4] $F(\omega)$ implicitly depends on T but $|F|^2/T$ is well–defined for $T \to \infty$.
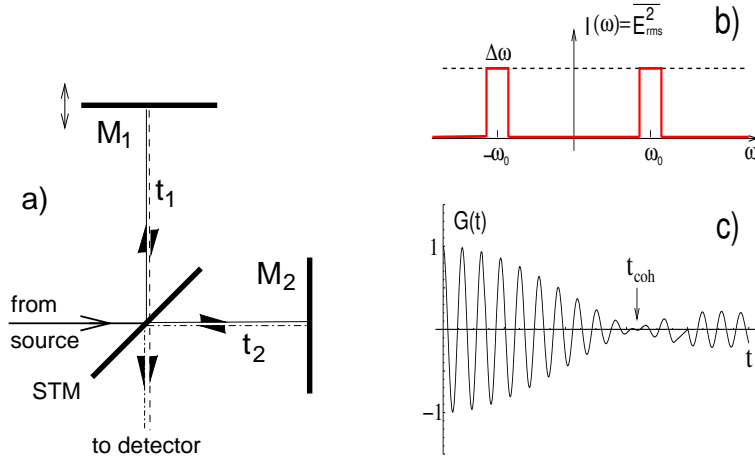
Figure 9. (a) Principle of a Michelson interferometer to measure the correlations in the optical electrical field, (b) filtered white noise, (c) coherence function.

$\mathcal{E}^{(\pm)}(t)$ denote the positive/negative frequency components of the optical electrical field $\mathcal{E}(t) = \mathcal{E}^{(+)}(t) + \mathcal{E}^{(-)}(t)$, see any book on quantum optics or Ref.[12].

4.3. SHOT NOISE

The thermionic current in a vacuum tube is not a smooth flow of electricity, but is subject to rapid and irregular fluctuations. These fluctuations, discovered by Schottky[16](a) (1918) and called by him "Schrot–Effekt" (small shot–effect) are caused by the random emission of (single) electrons from the cathode and are made manifest by voltage or current fluctuations in any circuit to which the tube is connected. If each emitted electron reaches the anode (saturation) within a neglectable transit time, the current will show–up as delta–spikes with Poissonian statistics (during fixed time), see Fig. 10(c).

– fluctuating current: $\qquad I(t) = \sum_k e\delta(t - t_k) = I_{\mathrm{dc}} + I_{\mathrm{n}}, \quad I_{\mathrm{dc}} = e\bar{n},$

– current corr. function: $\qquad C_{\mathrm{II}}(t) = e^2(\Delta n)^2\,\delta(t), \quad (\Delta n)^2 = \bar{n},$

– power spectrum: $\qquad C_{\mathrm{II}}(\omega) = \bar{n}e^2 = eI_{\mathrm{dc}}, \quad$ (white noise).

A bandwidth of $\Delta\omega$ contributes to the noise current (a factor 2 arises from the contributions at $\pm\omega_0$)

$$\text{Schottky–Formula:} \qquad \boxed{\; I_{\mathrm{rms}}^2 = 2eI_{\mathrm{dc}}\,\Delta\nu, \quad \Delta\nu = \Delta\omega/(2\pi). \;} \qquad (11)$$
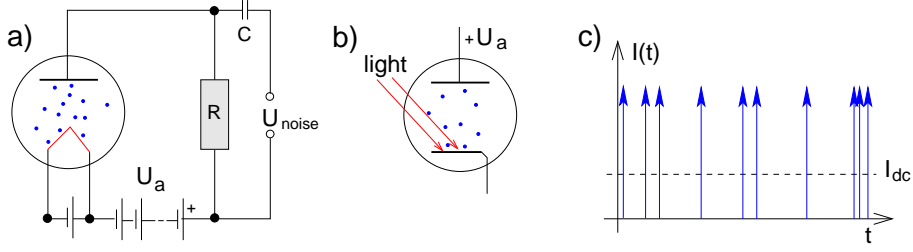
Figure 10. (a) Vacuum tube, (b) vacuum photo–cell, (c) shot noise current.

Example:
$$I_{dc} = 1\text{mA}, \quad \Delta\nu = 5\text{kHz}, \quad \leadsto I_{rms} = 1.3\text{nA}, \quad U_{rms} = 13\mu\text{V (at } R = 10k\Omega).$$
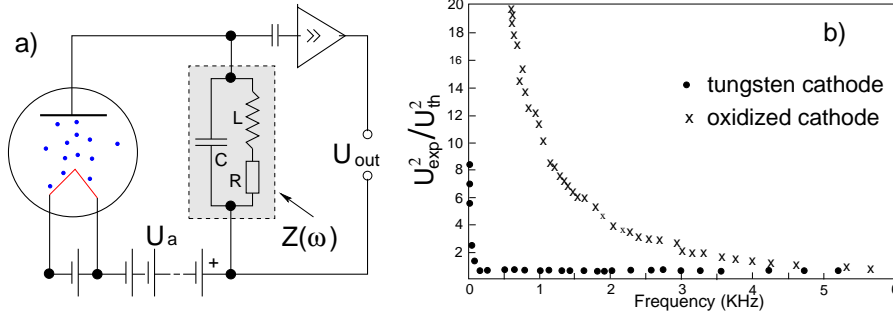

Figure 11. (a) Experimental set–up and (b) measured shot–noise power spectrum. $Z(\omega)$ is the impedance of the RCL circuit. The amplifier consisted of 5 tubes Western Electric 101/102D, RC–coupled with $U_{out} = 3 \times 10^5 U_{in}$. Redrawn from Ref.[16](b)

Fig. 11(a) sketches Johnson's experimental set–up[16](b) to measure the spectral dependence of the shot–noise from a vacuum tube by using a LC–resonance circuit, where $\omega_0 = 1/\sqrt{LC}$ and

$$U_{rms}^2 = \int_{-\infty}^{\infty} |Z(\omega)|^2 C_{II}(\omega)\,\frac{d\omega}{2\pi} = \frac{eI_{dc}}{2C^2}\left(\frac{L}{R} + RC\right).$$

Note, U_{rms} depends on the loss–resistance R, which had to be determined from the resonance curve of each LC circuit.

Thermionic emission from oxidized cathodes is more efficient than from pure metallic cathodes but it is more noisy ("1/f" noise), see Fig.11(b). In Quantum optics, shot noise is caused by fluctuations of the detected photons, e.g. in a vacuum photo–cell.
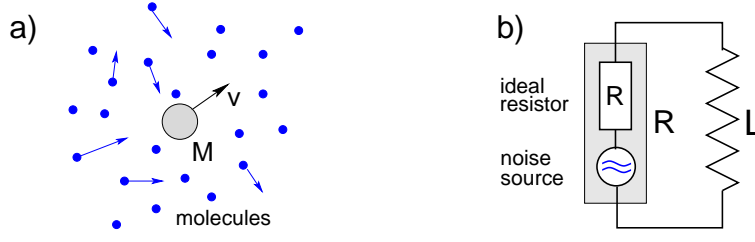
Figure 12. (a) Brownian motion of a particle in a fluid, (b) L–R circuit.

4.4. THERMAL NOISE (JOHNSON, NYQUIST, 1926)

The mechanism of noise–generation by a resistor at finite temperature T_0 is analogue to the *Brownian motion* of a heavy particle of mass M immersed in a fluid. The force of the molecules "pinging" on the Brownian particle consists of two parts: a frictional force $-\gamma' v$ and a stochastic force f_{st} which will be modelled by white noise. Remarkably, both parts are not independent but related by the *dissipation–fluctuation theorem*[17](b).

- Brownian motion: $\qquad M\dot{v} \quad = f_{\mathrm{total}} = -\gamma' v + f_{\mathrm{st}}(t),$

- velocity: $\qquad\qquad V(\omega) \quad = \frac{1}{M}\frac{1}{\gamma - i\omega} F_{\mathrm{st}}(\omega), \quad \gamma = \gamma'/M,$

- correlation function: $\quad C_{\mathrm{vv}}(\omega) \quad = \frac{1}{2T}|V(\omega)|^2 = |H(\omega)|^2\, C_{\mathrm{ff}}(\omega),$

- white noise: $\qquad\qquad C_{\mathrm{ff}}(\omega) \quad = \frac{1}{2T}|F(\omega)|^2 = \kappa =\text{const},$

- equipartion theorem: $\quad \dfrac{M}{2}\overline{v^2(t)} \;\; = \dfrac{M}{2}\int C_{\mathrm{vv}}(\omega)\dfrac{d\omega}{2\pi} = \dfrac{1}{2}k_{\mathrm{B}}T_0,$

- diss.–fluct. theorem: $\qquad\quad \kappa = 2k_{\mathrm{B}}T_0 M\gamma.$

The corresponding result for the LR–circuit is obtained by translating $v \to I, \quad M \to L, \quad \gamma \to R/L$, thus $C_{\mathrm{UU}}(\omega) = 2k_{\mathrm{B}}T_0 R$. This leads to the famous

Nyquist–Formula: $\qquad \boxed{\; U_{\mathrm{rms}}^2 = 4k_{\mathrm{B}}T_0 R\,\Delta\nu. \;}$ $\qquad\qquad$ (12)

This result can be generalized to an arbitrary impediance by $R \to \operatorname{Re} Z(\omega)$. Note, the equivalent circuit diagram of a real resistor consists of an ideal (noise–free) resistor with resistance R and a noise source with correlation function $C_{\mathrm{UU}}(\omega) = 2k_{\mathrm{B}}T_0 R$, see Fig. 12(b). Fig. 13 displays Johnsons original result.
Example:
$R = 1\mathrm{M}\Omega, \quad T_0 = 300\mathrm{K}, \quad \Delta\nu = 5\mathrm{kHz}, \quad \leadsto U_{\mathrm{rms}} \approx 2.5\mu\mathrm{V}.$

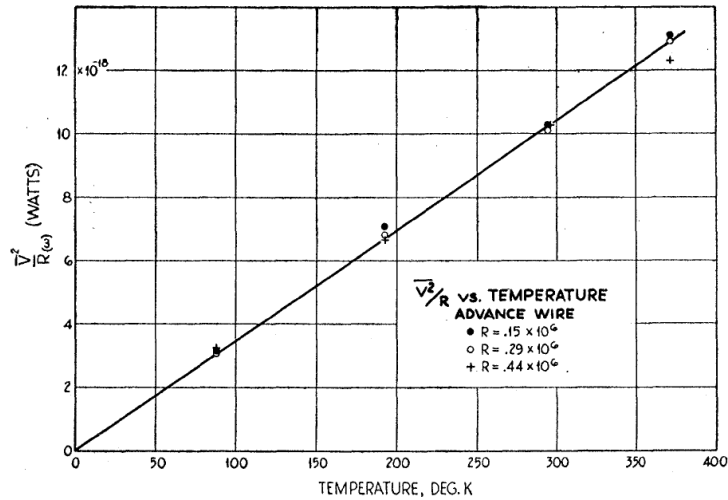*Figure 13.* Noise power U_{rms}^2/R generated by a resistor at temperature T_0[17](a).

5. Examples of Signal Extraction from Noise

5.1. BOX–CAR INTEGRATOR

The *Box–Car Integrator* (BCI) improves the S/N ratio by

– gating the detection (time window Δt),

– averaging over multiple pulses, S/N$\sim \sqrt{N}$,
  e.g. $N = 10^4$ improves S/N by 20dB.

Beginning with $t_0 = 0$, the "box–car" is shifted gradually to higher values so that the full signal dependence of the signal is covered, see Fig. 14. Today, BCI's are a standard tool in most physics laboratories.

Typical properties of commercially available instruments are

– integration time: $\Delta t = 2 \dots 15 \mu$s,

– number of samplings: $N = 1 \dots 10000$,

– trigger rate: dc$\dots$20kHz.

5.2. LOCK–IN AMPLIFIER

In its most basic form a *Lock–In Amplifier* (LIA) is an instrument with dual capability. It can recover signals in the presence of an overwhelming noise background or, alternatively, it can provide high resolution measurements of relatively clean signals over several orders of magnitude and frequency. (Modern instruments even offer more than these two basic functions).
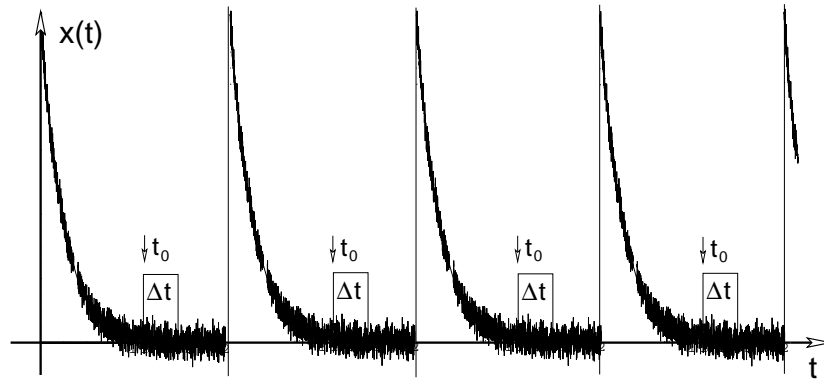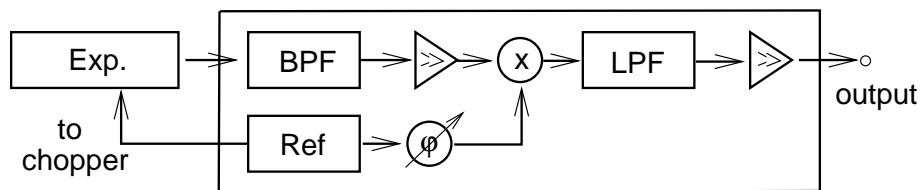
Figure 14. Principle of a Box–Car integrator.

Figure 15. Principle of a Lock–In amplifier. (BPF/LPF: band–pass/low–pass filter).

The LIA (in common with most ac indicating instruments) provides a dc output proportional to the ac input signal. In this method, one modulates (or chops) the input signal at a frequency appreciably above the information carrying frequency of the signal, amplifies at the modulation–frequency, and then synchronously demodulates this amplified output in order to recover the original signal information. The output of this *phase sensitive detection* is proportional to

$$\text{LIA:} \quad \boxed{C(\varphi, T) = \frac{1}{T} \int_0^T f(t) \sin(\omega t + \varphi) \, dt.} \tag{13}$$

T denotes the integration time and φ is the relative phase between the (sinusoidally) modulated signal and the reference. Thus, the LIA operates as an effective LPF with a bandwidth $\approx 1/T$.

Introductory articles about the lock–in technique may be downloaded from the web–pages of several companies, e.g. Refs. [18](a). In addition, there are numerous articles published in the American Journal of Physics about the physics and technique of lock–in laboratory experiments, e.g. Refs.[18](b-d).
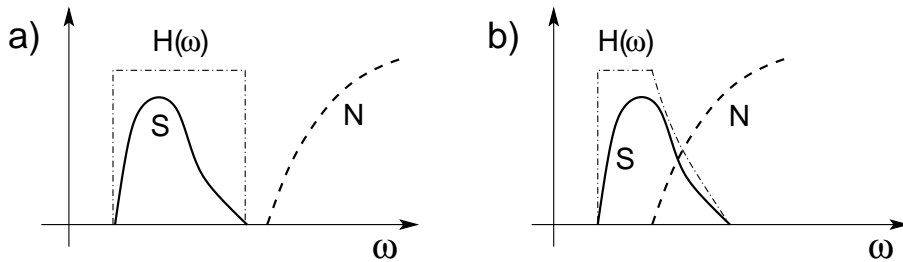
Figure 16. System function of a Wiener–Filter. (a) non–overlapping, (b) overlapping signal and noise spectra.

Commercially available instruments cover
– frequency range: 1mHz ... 2MHz ... ,
– voltage range: 2nV ... 1V,
– dynamics: 100dB.

An interesting "nostalgic" application can be found in the paper by Forrester et al.[19] about the detection of beats between two (incoherent) hyperfine transitions from Hg^{202} with an estimated S/N$\sim 3 \times 10^{-5}$. The crucial requirement was to maintain the total light intensity on the photocathode constant within 1×10^{-5} while modulating the beat–signal. This experiment also demonstrated that any time–delay between photon absorption and electron release must be significant less than 10^{-10}s.

5.3. WIENER–FILTER

We search for the optimum response function $H(\omega)$ of a linear filter which reproduces the useful (or expected) signal with greatest accuracy for given statistical properties of the signal and the noise, i.e. optimize $H(\omega)$ to minimize the error between the

– noisy signal $f(t) = s(t) + n(t)$ and the
– expected signal $g(t)$ $[=s(t),\ s(t-T),\dots]$.

If causality restrictions are ignored, minimalization of the quadratic–error between the filter output $x(t)$ and $g(t)$ in terms of $h(t)$ leads to the *Wiener–Equation*[2]

$$\int_{-\infty}^{\infty} h(t-t')\, C_{\mathrm{ff}}(t')\, dt' = C_{\mathrm{fg}}(t). \qquad (14)$$

$C_{\mathrm{ff}}(t)$ and $C_{\mathrm{nn}}(t)$, respectively, denote the auto–correlation functions of the signal output and the noise whereas $C_{\mathrm{fg}}(t)$ is the cross–correlation between signal–output and noise. Eq. 14 is of convolution–type and, thus, can be
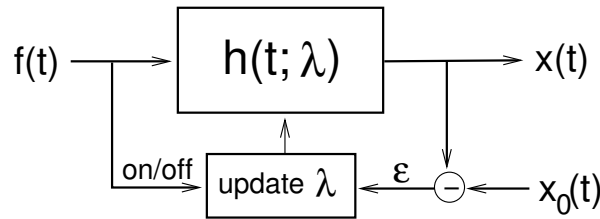
Figure 17. Sketch of an adaptive filter. $x_0(t)$ is a "training–signal" to adjust parameters.

solved by FT

$$H(\omega) = \frac{C_{\mathrm{fg}}(\omega)}{C_{\mathrm{ff}}(\omega)} \longrightarrow \frac{C_{\mathrm{ss}}(\omega)}{C_{\mathrm{ss}}(\omega) + C_{\mathrm{nn}}(\omega)}. \tag{15}$$

In the final result we assumed that signal and noise are uncorrelated. Fig. 16 sketches two examples.

5.4. ADAPTIVE FILTER

An adaptive filter – as sketched in Fig. 17 – is a filter which self–adjusts one or several parameters ("λ") of its response function according to an optimizing algorithm. (By contrast, the Wiener–filter is a static filter.)

In its simplest form, an adaptive filter is just a switch to select one of two possibilities. Teletype communication[20] provides a nostalgic example: Coding of "start" and "stop" of the 5-bit Baudot–coded letters is not uniquely determined (which matters when receiving secret, ciphered messages!). Therefore, a senseless training message was sent first which contained all letters: "The quick brown fox jumps over the lazy dog". From that, the operator found the correct position of the switch.

Some adaptive filters contain servo–motors as for the autofocus of a photo–camera. Because of the complexity of the problem, most adaptive filters are digital filters.

5.5. KALMAN–FILTER

The *Kalman–Filter* (KF) was invented in 1960 by Bucy and Kalman[21](a).

– First used in NASA's moon–landing navigation systems,

– now: integral part of autopilots, GPS–navigation, weather forecast[21](g)...

The hart of the KF is a set of recursive equations for the system variables $x(t)$ which provide a statistical estimate of the state from

– incomplete, noisy measurements (denoted by the M–comp. vector z),

– incomplete knowledge of a modelled system ("system noise").

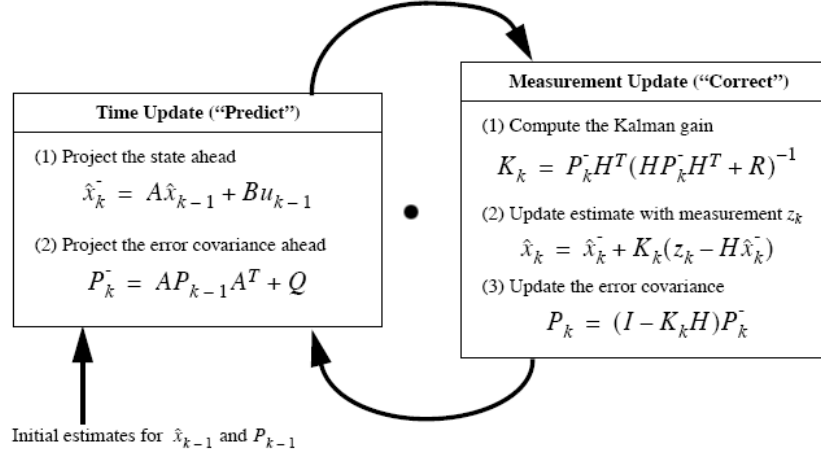[u is the "control", previously denoted by f].

Figure 18. The Kalman–Equations. From Welch & Bishop[21](b).

There are thousands of articles and dozens of books on the KF. From my point of view, the introductions given in Refs. [21](b-d) are of particular value to step into the field. We follow Welch and Bishop[21](b).

Process to be estimated:

system: $x_k = \mathbf{A}x_{k-1} + \mathbf{B}u_{k-1} + w_{k-1}$, ($k$: discrete time),

measurement: $z_k = \mathbf{H}x_k + v_k$,

noise: w, v denote the system and measurement noise, usually white Gaussian noise with covariances $\mathbf{R}(v)$, $\mathbf{Q}(w)$.

Estimates of system variables:

– a priori: $\hat{x}_k^-$, given x_k,

– a posteriori: $\hat{x}_k$, given z_k.

The Kalman–equation result from the minimalization of the error–squares of $\epsilon_k^- = x_k - \hat{x}_k^-$ and $\epsilon_k = x_k - \hat{x}_k$, see Fig. 18.

Example [Levy[21](e)]: determine the resistance of a given

– resistor: 100Ω, 2% acuracy,

– accuracy of Ohm–meter: $\pm 1\Omega$.

– System: $x_k = x_{k-1}$, $\quad \mathbf{Q} = 0$, ($\mathbf{A} = 1$),

– measurement: $z_k = x_k + v_k$, $\quad \mathbf{R} = (1\Omega)^2$, ($\mathbf{H} = 1$),

– best estimate: $x_0 = 100\Omega$, $\quad \sigma_R = P_0^- = (2\Omega)^2$ (without measurement).

Fig. 19 diplays a simulation of the measurement and its prediction of the correct value. Although the assumption of a Gaussian resistance–distribution
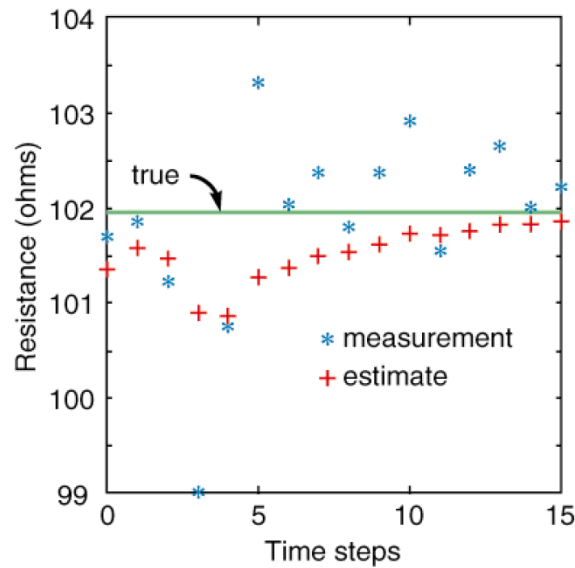
Figure 19. Series of measurements of the resistance of a resistor. From Levy[21](e).

is not very realistic, the results indicate that an analysis using statistical prediction algorithms is much better than simply taking the average of a series of measurements. Further examples can be found in Refs.[21](d,f,g).

5.6. SPEECH EXTRACTION FROM NOISE

Fig. 20 shows a typical speech signal. A characteristic feature is that the spectrum of its envelope function lays in the range $0.8 \ldots 7\mathrm{Hz}$. This distinguishes speech from many disturbing signals which may have overlapping power spectra and, therefore, cannot be de–entangled by a Wiener–filter. Nevertheless, extraction of the speech–component is possible, see Fig. 21 and audio–examples from the web-pages of the manufacturer[22](b).

Applications:
– long distance communication on short wave
  [atmospheric noise, crackling . . .]
– communication between a *Formula 1* pilot and his pitch box,
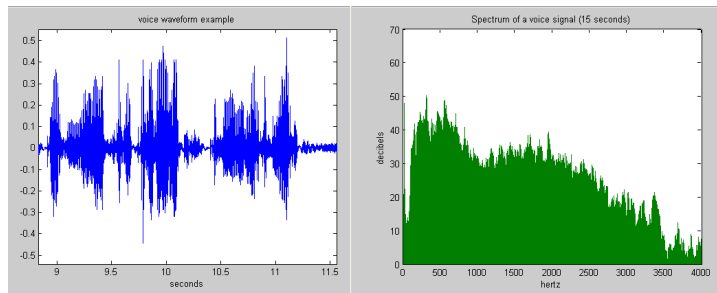 [uproar of engine, other cars,. . .].

Figure 20. A typical speech signal. Left: Time dependence, right: power spectrum[22](a).

Figure 21. Extraction of speech (right) from a noisy signal (left). From Ref.[22](b).

5.7. COCKTAIL PARTY PROBLEM

Consider a situation where there are N different signals $s_j(t)$ (within the same bandwidth) which are recorded as linear superpositions $x_i(t)$ (yet with unknown mixing ratios) by M different detectors. How to extract the $s_j(t)$? This is the field of *Independent Component Analysis* (ICA) also termed *Blind Source Separation* (BSS)[23](a,b).

Typical examples involving many sources and detectors are

– Cocktail–Party-Problem[23](a-c), see Fig. 22,

– separation of radar signals by an array of antennas[23](d),

– analysis of seismic signals[23](e),

– separation of biomagnetic sources, like electro–encephalograms (EEG)[23](f).

A simple situation occurs for two signals $s_1(t)$ and $s_2(t)$ (i.e. two "speakers"). The mixture of both signals reaches two microphones (i.e. two "ears" of another person) one wants to separate both sources

$$x_i(t) = \sum_{j=1}^{N=2} A_{ij} s_j(t), \quad i = 1 \ldots M(= 2).$$

Humans tackle the problem using the directivity of their ears, the known character of the voice in question, and their own "built–in personal com-

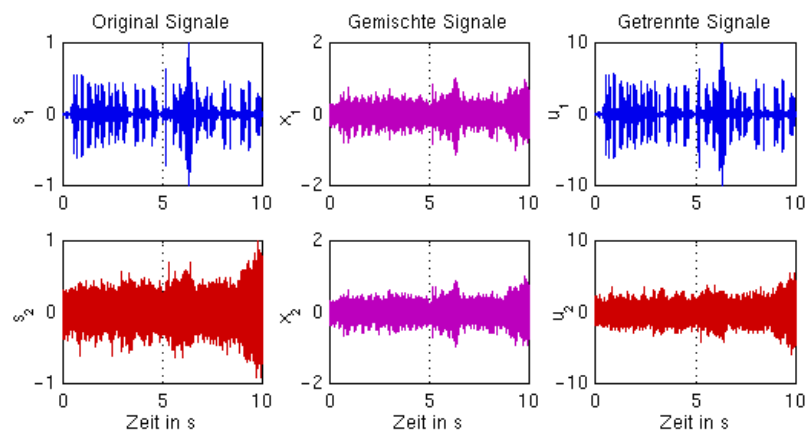*Figure 22.*   The Cocktail–Party problem: What did she say??

Figure 23.   Blind source separation of two signals[23](c).

puter". In contrast to the previous problem of chapts.5.6, several signals of the same type must be de–entangled.[5]

A surprising simple and powerful method to the problem can be found by claiming the statistical independence of the signals[23](a,c), i.e. minimizing the cross correlation between $u_1(t)$ and $u_2(t)$ in terms of W_{ij}

$$u_i(t) = \sum_{j=1}^{N} W_{ij} \ x_j(t).$$

The $u_i(t)$ represent a statistical estimate of $s_j(t)$, see Fig. 23.

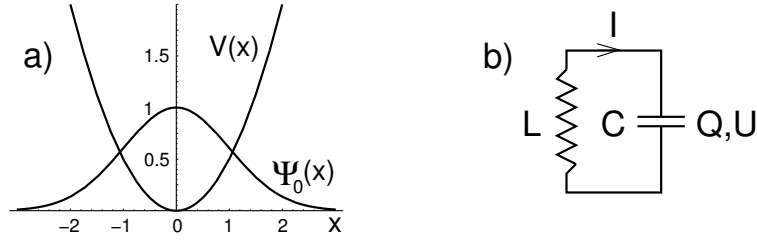[5] The mixing matrix $\mathbf{A}$ is unknown and possibly singular.

Figure 24.   (a) Particle in a parabolic potential, (b) LC–circuit.

6. Outlook: Quantum Noise

So far, noise was considered as a classical phenomenon. Shot noise from a vacuum tube (or vacuum photo–cell) stems from the discrete nature of the charge (or photon–energy) and, therefore, is ubiquitious in all phenomena detecting single electrons and photons. Johnson–Nyquist noise, on the other hand, originates from the thermal motion of the charge carriers and, hence, should classically dissappear in the limit $T_0 \to 0$. However, the momentum (or current–) operator (of an electron) is not a conserved quantity, so that the current must fluctuate even at $T_0 = 0$K , i.e. in the ground state of the system. This is called *Quantum–Noise.*

6.1. NON–DISSIPATIVE SYSTEMS

– Harmonic oscillator: $\hat{H} = \dfrac{\hat{p}^2}{2m} + \dfrac{1}{2}m\omega_0^2\,\hat{x}^2,$

– eigenstates: $|n\rangle,\; n = 0, 1, 2, \ldots, \quad E_n = (n + \tfrac{1}{2})\hbar\omega_0,$

– x-fluctuations: $\Delta x = \sqrt{\dfrac{\hbar}{2m\omega_0}(1 + 2n)},$

– LC circuit: $x \to Q, \quad m \to L,$

– voltage fluctuations at C: $\Delta U = \dfrac{\Delta Q}{C} = \sqrt{\dfrac{\hbar\omega_0}{2C}(1 + 2n)},$

– thermal equilibrium: $n \to \bar{n} = \dfrac{1}{e^{\hbar\omega_0/k_\mathrm{B}T_0} - 1}.$

Example:
C=10 pF,   L=0.25μH, $\nu_0 = \omega_0/2\pi = 100$MHz.
At $T_0 = 0$ K: $\Delta Q = 4.5$e (1500e), $\Delta U = \Delta Q/C = 70$nV (25$\mu$V).
Values in parenthesis hold for room temperature $T_0 = 300$K. Note, these fluctuations are not small, however, they originate from a rather broad band.
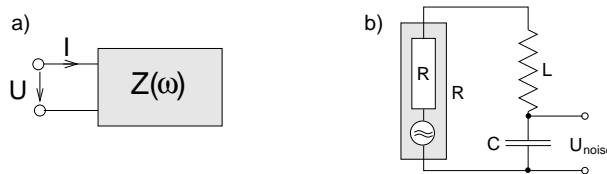
Figure 25. (a) Voltage fluctuations: (a) at impedance Z, (b) at a RCL circuit.

6.2. DISSIPATIVE QUANTUM SYSTEMS IN EQUILIBRIUM

There is no Hamiltonian of a damped system, hence, the quantum mechanical treatment of dissipationis nontrivial and must explicitly include the degrees of freedom of the heat bath[24](a). Nevertheless, Callen and Welton[24](b) discovered that in linear response theory the Nyquist-result (12) can be generalized to all quantum systems in thermal equilibrium (Quantum Dissipation Fluctuation Theorem, QDFT), see also Ref. [24](c)

$$
\text{QDFT:} \quad \boxed{C_{\mathrm{UU}}(\omega) = \hbar\omega \coth\left(\frac{\hbar\omega}{2k_{\mathrm{B}}T_0}\right) \operatorname{Re} Z(\omega).}
\tag{16}
$$

$Z(\omega)$ is the impedance (without noise source) at the port of the system where the voltage fluctuations are considered, see Fig. 25(a). Note, that this is "blue noise" rather than white noise! For $k_{\mathrm{B}}T_0 \gg \hbar\omega$, Eq. (16) conforms with (12).

Example: voltage fluctuations at the capacitor of Fig. 25(b):

$$
U_{\mathrm{rms}} = \sqrt{\frac{\epsilon_0}{C}}, \quad \epsilon_0 = k_{\mathrm{B}}T, \ (k_{\mathrm{B}}T_0 \gg \hbar\omega_0), \quad \epsilon_0 = \frac{1}{2}\hbar\omega_0, \ (k_{\mathrm{B}}T_0 \ll \hbar\omega_0 \ll \hbar/RC).
$$

In the classical limit, $k_{\mathrm{B}}T_0 \gg \hbar\omega_0$, U_{rms} is independent of R.

6.3. HOW TO BEAT SHOT NOISE?

The dection of gravitational waves is still one of the most challeging problems in physics[25](a). The relative accuracy needed for detection is 10^{-21}! Even at very high light intensities the Poissonian statistics of the detected Laser–photons may be relevant, see Fig. 26.

The quantum state of an ideal single mode laser is described by so-called "α–states" (coherent states, Glauber—states). In terms of the photon number eigenstates $|n\rangle$ we have

$$
|\alpha\rangle = e^{-\frac{1}{2}|\alpha|^2} \sum_{n=0}^{\infty} \frac{\alpha^n}{\sqrt{n!}} |n\rangle.
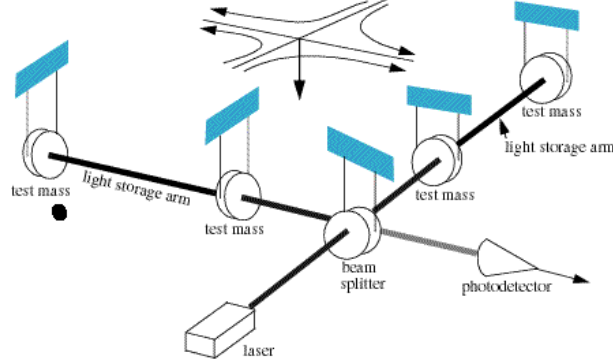\tag{17}
$$

Figure 26. Sketch of a Michelson–type gravitational wave detector. From Ref.[25](a).

$\alpha = |\alpha|e^{i\phi}$ is a complex number. In such a state the photon–distribution is a Poissonian with mean $\bar{n} = |\alpha|^2$. The expectation value of the optical electrical field is identical with a classical monochromatic plane wave

$$\langle \hat{\mathcal{E}}(t) \rangle \propto |\alpha| \, \sin(\mathbf{kr} - \omega t - \phi).$$

Therefore, the detection of photons is limited by "classical" shot noise. The number states, on the other hand, do not show photon–noise but they are extremely nonclassical and not related to sinusoidal waves which are needed in an interferometer. Nevertheless, there are states with sub–Poissonian statistics which are "in between" α–states and photon number states[25](b) or Ref.[12]. Recently, the first successful experiment using *squeezed states* has been published demonstrating that photon detection 2.8dB below the shot noise limit is posssible[25](c).

NB: Spatially noiseless optical amplification of images was recently demonstrated by a french group[26].

7. Acknowledgements

8. Appendix A

The following Huygens–to–earth radio link parameters have been taken from Folkner et al.[4](b) to estimate the signal and noise voltages at the receiver at the Green Bank Telescope (GBT) in West Virginia, USA. The ultrastable signal at 2.040 GHz was down–converted to 300kHz and sampled at a rate of 1.25Mhz with 8 bit resolution.

– distance Titan – Earth: $\quad d \quad \approx 8\text{AU}, \quad (1\text{AU} \approx 150 \times 10^6 \text{km})$,

– Huygens radiation power: $P \quad = 10.6\text{W}, \ (3\text{dB beam width: }120\text{degree})$,

– at GBT receiver: $\qquad\qquad P_{\text{in}} \ \approx 2.8 \times 10^{-21}\text{W}$,

$\qquad\qquad\qquad\qquad\qquad U_{\text{in}} \ = 3.7 \times 10^{-10}\text{V}, \quad (\text{at } R = 50\Omega)$,

– thermal noise: $\qquad\qquad U_{\text{rms}}^2 = 4\,k_{\text{B}}T_0\,R\,\Delta\nu, \ (\Delta\nu = 1\text{Hz}, \ T_0 = 30\text{K})$,

– power–matching: $\qquad\qquad U_{\text{noise}} = U_{\text{rms}}/2 \approx 1.4 \times 10^{-10}\text{V}$,

$\qquad\qquad\qquad\qquad\qquad P_{\text{noise}} = U_{\text{noise}}^2/R = 1.6 \times 10^{-21}\text{W}$.

– estimated S/N ratio: $\qquad S/N \approx 8\text{dB}$.

References

1. (a) A. V. Oppenheim and A. S. Willsky, eds. (1983), *Signals and Systems*, Prentice Hall;
   (b) J. L. Lacoume et al., eds. (1987), *Signal Processing*, North Holland;
   (c) http://en.wikipedia.org/wiki/Signal_processing.
2. L. A. Wainstein and V. D. Zubakov (1962), *Extraction of Signals from Noise*, Prentice Hall.
3. (a) http://www.gb.nrao.edu/GBT/GBT.shtml; http://www.nrao.edu/news/newsletters/;
   (b) http://en.wikipedia.org/wiki/Green_Bank_Telescope.
4. (a) M. K. Bird et al. (2006), NRAO Newsletters **107**, 3, see Ref. [3](a);
   (b) W. M. Folkner et al. (2006), J. Geophys. Res. **111**, E07S02;
   (c) M. K. Bird, personal communication.
5. *Cassini Huygens – Huygens Probe Mission Description* (Dec. 2004),
   Jet Propulsion Laboratory, CALTEC, JPL D-5564, Rev. O (suppl., ver. 2).
6. (a) Moon reflection signals (EME): http://www.moonbounce.info/wav.html;
   (b) Mars Global Surveyor Relay Test:
       http://ourworld.compuserve.com/homepages/demerson/.
7. (a) http://en.wikipedia.org/wiki/Fourier_transform;
   (b) http://en.wikipedia.org/wiki/Discrete_Fourier_transform.
8. (a) http://www.h-wolff.de/;
   (b) http://www.w1vd.com/;
   (c) http://www.w1tag.com/.
9. W. H. Press et al. (2003), *Numerical Recipes in C*, Cambridge.
10. H. Babovsky et al. (1987), *Math. Methoden der Systemtheorie: Fourieranalysis*, Teubner.
11. Telefunken A.G. (1963), *Mechanische Filter*, Telefunken Zeitung Jg. **36**, Heft 5, 275.

12. R. v. Baltz (2005), *Photons and Photon Statistics: From Incandescent Light to Lasers*. In: *Frontiers of Optical Spectroscopy*, B. Di Bartolo and O. Forte, eds., Springer.

13. R. Landauer (1998), Nature **392**, 658.

14. (a) N. G. van Kampen (1983), *Stochastic Processes in Physics and Chemistry*, North Holland;
    (b) http://en.wikipedia.org/wiki/Statistics.

15. (a) J. L. Passmore et al. (1995), Am. J. Phys. **63**, 592;
    (b) Y. Kraftmakher (1995), Am. J. Phys. **63**, 932;
    (c) W.T. Vetterling and M. Andelman (1979), Am. J. Phys. **47**, 382.

16. (a) W. Schottky (1918), Ann. Phys. (Leipzig), **57**, 541;
    (b) J. B. Johnson (1925), Phys. Rev. **26**, 71.

17. (a) J. B. Johnson (1928), Phys. Rev. **32**, 97;
    (b) H. Nyquist (1928), Phys. Rev. **32**, 110.

18. (a) Perkin Elmer: http://www.cpm.uncc.edu/lock_in_1.htm;
    (b) R. Wolfson (1991), Am. J. Phys. **59**, 569;
    (c) J. H. Scofield (1994), Am. J. Phys. **62**, 129;
    (d) K. G. Libbrecht et al. (2003), Am. J. Phys. **71**, 1208.

19. A. Th. Forrester et al. (1955), Phys. Rev. **99**, 1691.

20. http://en.wikipedia.org/wiki/Teleprinter.

21. (a) R. E. Kalman, Trans. ASME J. Basic Eng. **82**(Series D), 35 (1960);
    (b) G. Welch and G. Bishop, *An Introduction to the Kalman–Filter*,
        http://www.cs.unc.edu/~welch/kalman/index.html;
    (c) P. D. Joseph, http://ourworld.compuserve.com/homepages/PDJoseph/;
    (d) R. Webster and G. B. M. Heuvelink (2006), Eur. J. Soil Sci. **57**, 758;
    (e) L. J. Levy, http://www.cs.unc.edu/~welch/kalman/Levy1997/index.html;
    (f) D. Simon, *The Kalman Filter: Navigation's Workhorse*,
        http://www.innovatia.com/software/papers/kalman.htm;
    (g) D. Mackenzie (2003), SIAM News **36**, No. 8.

22. (a) Found somewhere on the WWW;
    (b) http://www.Ing-Michels.de.

23. (a) Hyvärinen, A. et al. (2001), *Independent Component Analysis*, Wiley;
    (b) http://en.wikipedia.org/wiki/Cocktail_party_effect;
        http://en.wikipedia.org/wiki/Blind_signal_separation;
    (c) K. R. Müller: http://www.first.fraunhofer.de/ida;
        http://ddi.cs.uni-potsdam.de/HyFISCH/Spitzenforschung/Mueller.htm;
    (d) F. Cristopher and C. Morrisean (1985), Proc. Xeme Coll. GRETSI, 1017;
    (e) S. Williamson et al., eds. (1990). *Advances in Biomagnetism*, Plenum;
    (f) F. Acernese et al. (2003), IEEE Trans. Neur. Netwks. **14**, 167.

24. (a) T. Dittrich et al., eds. (1998), *Quantum Transport and Dissipation*, Wiley-VCH;
    (b) H. B. Callen and T. A. Welton (1951), Phys. Rev. **83**, 34;
    (c) L. Banyai (1985), Z. Phys. B **58**, 161.

25. (a) http://en.wikipedia.org/wiki/Gravitational_wave;
    (b) R. E. Slusher and B. Yurke (1988), *Unterdrückung des Quantenrauschens bei Lichtwellen*, Spektrum der Wiss., Juli–Heft, S. 70, (Sci. Am., June 1988?);
    (c) H. Vahlbruch et al. (2005), Phys. Rev. Lett. **95**, 211102.

26. A. Mosset et al. (2005), Phys. Rev. Lett. **94**, 223603.